WPPMI-CPR(17) 17633

Yu. L. Igitkhanov et al.

Effects of 3D Divertor Performance on the Pumping Efficiency in DEMO

Preprint of Paper to be submitted for publication in Proceeding of 13th International Symposium on Fusion Nuclear Technology (ISFNT)

This work has been carried out within the framework of the EUROfusion Consortium and has received funding from the Euratom research and training programme 2014-2018 under grant agreement No 633053. The views and opinions expressed herein do not necessarily reflect those of the European Commission.

Effects of 3D Divertor Performance on the Pumping Efficiency in DEMO

Stylianos Varoutis[a], Yuri Igitkhanov[a], Christian Day[a], Holger Strobel[a] and Ronald Wenninger[b,c]

[a]Karlsruhe Institute of Technology (KIT), Institute for Technical Physics, Karlsruhe, Germany
[b]EUROfusion Programme Management Unit, Garching, Germany
[c]Max-Planck-Institute for Plasma Physics (IPP), Garching, Germany

Abstract

In this paper we analyze the pumping efficiency of a generic 3D DEMO divertor configuration based on the size of inter-cassette gaps. Due to symmetry conditions we consider only one segment, which is composed by 3 divertor cassettes with the pumping port located at the bottom of the middle cassette and with four inter-cassette gaps. The width of inter-cassette gaps or the number of pumping ports is defined by the requirement to minimize the outflow of particles from the divertor to the plasma and hence, the highest possible pumping efficiency for the particle throughput, expected in DEMO, to be achieved. The DIVGAS code is used to perform a sensitivity analysis of the pumping efficiency, defined as a ratio of pumped particles to the particle throughput for different inter-cassette widths. The analysis shows that for the reference case of 20 mm a reduction on the pumping efficiency of the order of 10% is observed when compared with the case of a completely sealed divertor. For smaller gaps the pumping reduction is found to be negligible, while for large values of the gap width the pumping reduction may reach the value of 20%. Furthermore, almost 80% of the incoming particles are moving towards the x-point, independent of the gap width. Therefore, the gap width does not influence the outflux towards the x-point, but only strongly affects the pumping efficiency. This analysis is meant to contribute to the ongoing DEMO divertor design efforts.

Keywords: DEMO reactor, divertor, pumping, fueling, neutral modelling

1. Introduction

One of the important aspects of DEMO divertor and the first wall design is the presence of gaps between the divertor cassettes, which cannot be sealed perfectly due to technical constraints. As a consequence, unintended particle fluxes will occur both in poloidal and toroidal direction and between the divertor cassettes. This issue has been already investigated for the case of Alcator C-Mod [1], in which the influence of the gaps in the poloidal and toroidal direction is significant and only if their existence is assumed, the corresponding numerical and experimental results may coincide. Furthermore, the same study has been performed for the case of ITER [2], where the simulations indicate that there is no major negative effect of the gaps on the divertor performance, although the parasitic flows caused by these gaps can be comparable to the pumping throughput. To the best of the authors' knowledge, there isn't any other study, which investigates the influence of the gaps in a systematic way and for several values of gap width. The only work, which describes in brief the influence of the gaps considering more than one gap width case, namely 10mm and 20 mm, is Ref. [3], which is focused on the ITER divertor. There, it has been found that for the burn phase a very strong back streaming of gas into the plasma, mainly caused by the flows in the gaps between the cassettes, takes place. Following, the aforementioned studies, in the present work a three dimensional model of the DEMO divertor has been developed and simulated in order to investigate the influence of the gaps to the DEMO pumping efficiency, defined as a ratio of pumped particles to the total incoming particle throughput. The actual model of a DEMO divertor segment with the pumping port to be positioned at the bottom of the middle cassette is shown in Fig.1. The depicted divertor configuration is based on the 2015 EU DEMO baseline design [4], which consists of 54 divertor cassettes in total.

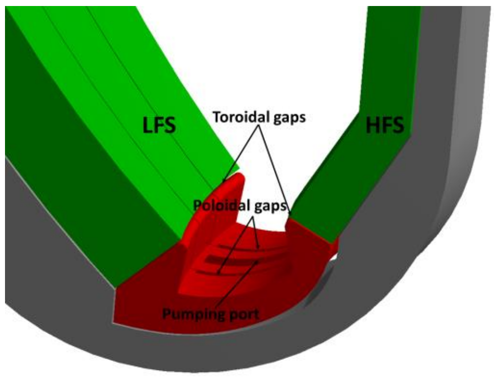

Fig. 1. Three dimensional DEMO 2015 divertor configuration including three divertor cassettes as well as the pumping port slot at the bottom, the first wall with low field side (LFS) and high field side (HFS) and the surrounding vacuum vessel.

Due to toroidal symmetry we consider only one sector of 20°, which includes 3 divertor cassettes without the dome structure, two poloidal gaps between the cassettes (i.e inter-cassette gaps) and two toroidal gaps between the first wall and the divertor cassettes in both the low field and high field sides (LFS and HFS). Furthermore, a pumping port is considered and is located in the middle cassette occupying the whole bottom part of the structure. All the gaps are interconnected and lead

author's email: stylianos.varoutis@kit.edu

to the pump entrance, which is located below the end of the pumping port. In the present work, the width of all aforementioned gaps consists of the main input parameter of the analysis and is defined by the requirement to minimize the outflow of particles from the divertor into the plasma and hence, the highest possible pumping efficiency to be achieved in DEMO.

The primary goal of this paper is to model the gas flow in the volume, which extends between the divertor cassettes, the vacuum vessel and the first wall and to explore the effect of the neutral flux through the gaps onto the DEMO divertor pumping efficiency and the possible need of additional sealing. For this purpose, the DIVGAS code [5], which describes the neutral particle transport for arbitrary collisionality regime has been implemented. The code is based on the Direct Simulation Monte Carlo (DSMC) method [6] and estimates the distribution of macroscopic parameters of neutrals in the whole flow domain as well as the flow pattern, the pumped particle flux and the particle flux through the inter-cassette gaps and through the private flux region towards the plasma.

The analyses of the influence of the inter-cassette gaps on the overall pumping efficiency are meant to contribute to the ongoing DEMO divertor design efforts. The schematic model taking into account the gas leaks between the divertor components is described in section 2, the 3D modelling results upon application to DEMO are shown in section 3, and conclusions are drawn in section 4.

2. Numerical model

2.1 The 3D divertor geometry

In order to allow for better mesh generation, the divertor configuration as shown in Fig.1 was slightly modified. Five different geometrical configurations were extracted, namely a configuration without gaps and four configurations, in which the width of the gaps takes the following values: 10 mm, 20 mm, 30 mm and 40 mm. In Fig. 2, the case without gaps is presented, where the transparent surfaces A and B in the HFS and LFS correspond to the virtual windows, through which neutrals penetrate the private flux region and on which the incoming boundary conditions are imposed. The corresponding area for each surface is 1.6 m^2 and 2.8 m^2 respectively. The surface C represents the boundary through which the neutrals will be immediately ionized and removed from the flow domain and it is extended to the toroidal direction. The area of surface C is 1.7 m^2. It is noted that, all the above surfaces remain fixed for all the geometrical configurations examined here further. Additionally, in Fig. 2, it is shown that the pumping port is extended downwards and its cross-section has a total area of 0.5 m^2. In the case of the design without gaps, it is assumed that the particles, which flow through the pumping port, will be pumped out by the bottom surface of the pumping port, on which a given capture coefficient (cf section 2.2 below) is appointed.

In Fig. 3, the 3D DEMO divertor configuration, which corresponds to a 20^o sector and includes toroidal and poloidal gaps is shown. For representation purposes, the cut along the plane DD´ is additionally presented. It is noted that in all simulations only the middle pumping port is considered, while the two neighboring ports/openings, for simplicity purposes, are completely neglected. In this specific design, the particles, which enter the pumping port and reach its outlet, have the possibility to flow in the toroidal or poloidal direction in the volume between the divertor cassette and the vacuum vessel. The adsorbing surface in this case is located further below the pumping port outlet, and based on the CAD file, coincides with the pumping slot of the vacuum vessel. As previously, a given capture coefficient for the pumping slot is appointed.

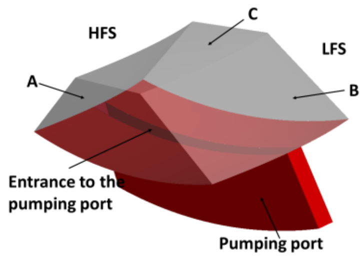

Fig. 2. 3D DEMO divertor geometry without gaps in the toroidal and poloidal directions.

More specific, in Fig. 4a, a cut of the divertor model along the DD´ plane is shown. In this cut the considered toroidal and poloidal gaps are presented, as well as the vacuum vessel and the pumping port. Moreover, the pumping slot located at the vacuum vessel, is depicted. A bottom view angle of the model is shown in Fig 4b, at which the pumping slot is highlighted. The total area of the pumping slot is equal to 2 m^2.

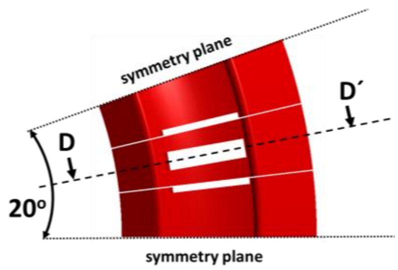

Fig. 3. A 20^o divertor sector is presented. Here only the middle pumping port is considered. A cut along the plane DD´ as well as the symmetry planes is shown.

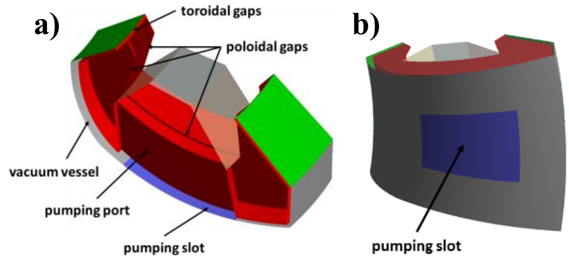

Fig. 4. a) A cut along the plane DD´ (shown in Fig.3), in which the toroidal and poloidal gaps, the vacuum vessel, the pumping port and the pumping slot are shown. b) A bottom view angle of the model.

2.2 Numerical approach and boundary conditions

Since DSMC has been proven to be a reliable numerical tool to describe the behavior of rarefied gases in the divertor area, detailed description of this method here is omitted and the reader may refer to the following publications [7-9] for further details. In the present work only the essential aspects of the implementation are mentioned. Briefly, the simulated number of particles for all calculations ranges between $1x10^7$ to $2x10^7$, while the time step is equal to Δt=1μs. For all cases, an unstructured tetrahedral mesh has been implemented. The resulted numerical grid shown in Fig. 5 can be obtained, if a cut along the DD′ plane (see Fig. 3) is applied. The total number of the computational cells is of the order of $2x10^6$. Each simulation needs several weeks for reaching steady state conditions by using an HPC and in particular 200 CPUs for each run. For all simulated cases the particle balance of the total incoming and outgoing particles in the flow domain is satisfied.

Fig. 5. Presentation of the unstructured tetrahedral computational grid applied in DIVGAS simulations.

In the present model, the neutral deuterium flux entering the private flux region is defined by specifying the pressure and the temperature at the entrance to the private flux region (PFR). In particular, the plasma D ions are neutralized on the vertical divertor plates and as D_2 molecules penetrate the PFR (He or T molecules can be treated in similar fashion in the model) with reference pressure P_0 and temperature T_0 equal to 1 Pa and 4023 K (or 0.35 eV) respectively. The applied boundary conditions of pressure and temperature for molecular deuterium correspond to an ITER relevant detached plasma scenario as described in [10,11]. It is noted that in the present work the ionization, dissociation and recombination processes on the walls or in the gas phase are not taken into account. Therefore, when a deuterium molecule hits a stationary wall, it remains as molecule and a purely diffuse reflection takes place, where the incident molecule is reemitted with Maxwellian distribution based on the wall temperature, equal to T_{wall}=420 K. In the case of a particle intersecting with the pumping surface, it can be completely removed from the computational domain according to a certain probability, which is given by the capture coefficient ξ. Consequently, ξ takes values between $0\leq \xi \leq 1$. It is noted that ξ represents the imposed condition of fixed pumped particle flux and is related with the effective pumping speed of the pumping surface. In the present work the capture coefficient takes the following values, namely ξ=0.1, 0.3, 0.6, 1. If the particle is not finally absorbed from the pumping surface, then the particle undergoes a diffuse reflection, assuming that the temperature at the entrance to the pump is equal to 420 K. Additionally, when a particle goes through the toroidal and poloidal gaps (shown in Fig. 4) as well as the dome structure then, an expansion into vacuum is considered resulting in the complete particle removal. The latter assumption can be justified, since an interaction with the plasma takes place and results in the immediate neutral particle ionization. Finally, when a particle intersects with one of the symmetry planes, as shown in Fig. 3, then the particle undergoes a specular reflection and preserves its kinetic energy.

3. Results and discussion

In Fig. 6, the fraction of fuel particles pumped out due to the gaps as a function of gap width is shown for four values of the capture coefficient ξ. This ratio has the same behavior with the previously defined pumping efficiency. It is seen that, as the gap width increases, the pumped out fraction decreases. For small values of ξ, this reduction seems to be more significant. In particular, for the reference case of a 20 mm gap, the pumping efficiency reduction is maximum 10% and depends on ξ. For the case of 10 mm width, it is observed that the pumping reduction does not depend on the gap width and consequently for gap widths less or equal to 10 mm, the divertor can be considered as sealed. For larger values of gap width, the pumping reduction is even more significant and a maximum value of 20% was found for the maximum investigated gap width of 40 mm. It is noted that the estimated ratio does not take into account the particle losses towards the x-point.

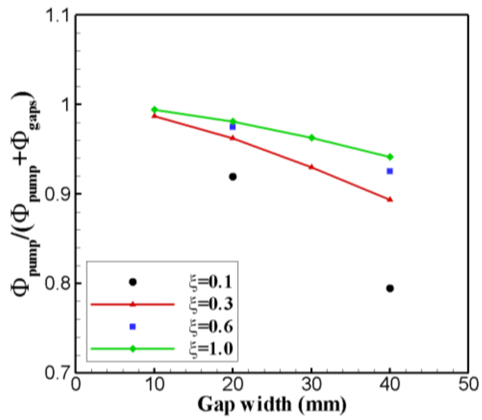

Fig. 6. Reduction of pumped out fraction of fuel particles due to the gaps as a function of the gap width.

In Fig. 7, the ratio of the total particle flux going through the gaps and back to SOL to the pumped out flux in the case without gaps as a function of the gap width is presented. This ratio represents the influence of the gaps in the pumping efficiency and in general the higher this ratio, the smaller the divertor pumping efficiency. More specific, it is observed that in the reference case of 20 mm, the ratio varies between 2% and 15%, which shows that in the worst case 15% of the particle flux flows through the gaps and penetrates the SOL. The rest of the particles either will be pumped out or move towards the x-point. In the case of 40 mm gap and for ξ=0.1, the ratio is equal to 50%, which means that half of the total incoming particles will flow back to the SOL and will not be finally pumped. In reality, it is expected that there is going to be an influence of the escaped particles to the incoming boundary conditions, but such an effect will be considered only in a future investigation.

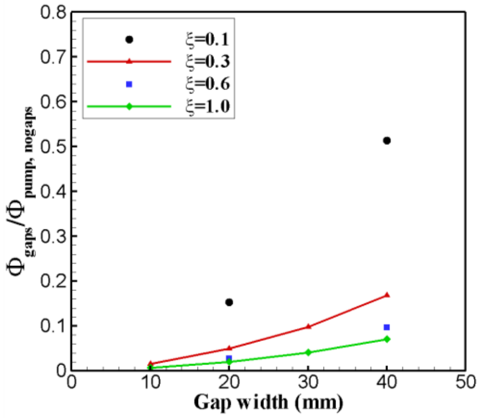

Fig. 7. Ratio of particle flux through the gaps and the pumped flux in the case without the gaps as a function of gap width.

In Fig. 8, the normalized outflux of particles, which escape the flow domain and move towards the x-point, as a function of gap width is depicted. The normalization of outflux is based on the total net particle flux, which enters the PFR. It is clearly seen that for the given configuration without the dome, the outflux is independent of the gap width, while a small dependence on ξ is observed. The existence of gaps do not influence the outflux towards the x-point but strongly affect only the pumped particle flux. Here it should be noted that the imposed boundary conditions are kept fixed, whereas in principle the particles, which escape to the PFR, affect the incoming boundary conditions by considering their reentry to the PFR. A more realistic representation would be to assume variable incoming boundary conditions of molecular deuterium, which will lead to

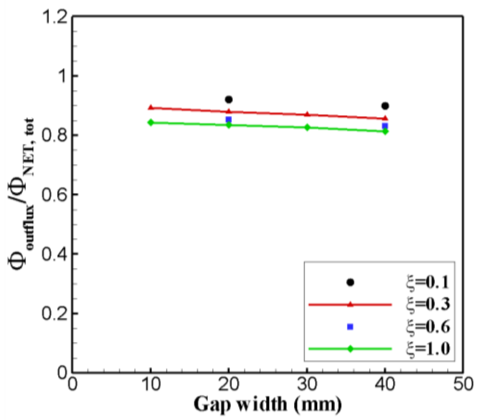

Fig. 8. Normalized particle outflux as a function of gap width.

the increase of the outflux and the corresponding pumped flux. Since the particle loss towards the x-point prevails all other particle losses in the divertor, the actual dependence of pumping efficiency on the gap width is not so critical. For the reference case of 20 mm, the outflux is ~82% of the total net incoming particles. This conclusion indicates that there is a necessity towards a study, which takes into account the dome structure in order a more precise definition of the actual role of gaps on the pumping efficiency to be assessed.

In Fig. 9, a representative pressure contour and the corresponding streamlines for the case of a gap width of 40 mm and a capture coefficient of ξ=1 are presented. It is seen that the particle move is fully justified by the local pressure drop. The particle flow creates a very complex pattern, which is extended around the divertor cassettes and through the divertor gaps. The present flow case is an indicative example, while the same qualitative behavior was found in the other simulations as well.

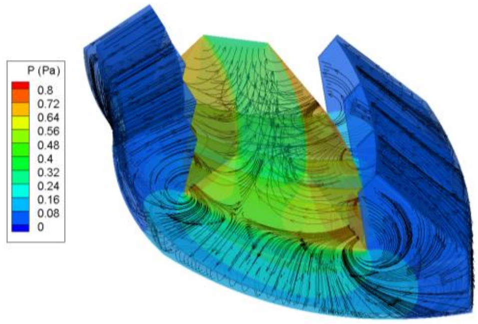

Fig. 9. Pressure contour and streamlines for the case of gap width 40 mm and capture coefficient equal to ξ=1.

4. Conclusions

The results of DIVGAS modelling of the three dimensional 2015 DEMO divertor design is considered in the present work. The effect of gas leaks between the divertor cassettes is assessed, and a sensitivity analysis of the results on the divertor geometry and on the inter-cassette gaps is conducted.

The analysis shows that the pumping efficiency depends on the gap width, and for the reference case of 20 mm there results a reduction on the pumping efficiency up to 10%. For smaller values of the gap width the pumping efficiency reduction was found to be negligible, while for larger values of the gap width the pumping efficiency reduces further (up to 20% for a 40 mm gap).

In the present configuration almost 80% of the incoming particles are moving towards the x-point, independent of the gap width. Therefore, the gap width does not influence the outflux towards the x-point, but only strongly affects the pumping efficiency. Previous work done for the ITER divertor with dome revealed a stronger influence of the gaps [3]. Hence, as future work, the same parametric analysis as shown above but taking into account the dome structure will be performed in order to eliminate the influence of the outflux so that the effect of gaps on the pumping efficiency will be revealed in a more pronounced way.

The analyses of the influence of the inter-cassette gaps on pumping efficiency are meant to contribute to the ongoing DEMO divertor design efforts.

Acknowledgments

This work has been carried out within the framework of the EUROfusion Consortium and has received funding from the Euratom research and training programme 2014-2018 under grant agreement No 633053. The views and opinions expressed herein do not necessarily reflect those of the European Commission.

Part of this work was performed by using computational resources provided by the MARCONI-FUSION HPC. The rest of this work was performed on the computational resource bwUniCluster funded by the Ministry of Science, Research and Arts and the Universities of the State of Baden-Württemberg, Germany, within the framework program bwHPC.

References

[1] D.P. Stolter, B. LaBombard, “Three-dimensional simulation of gas conductance measurement experiments on Alcator C-Mod”, J. Nucl. Mater. vols. 337–399, pp. 510–514, 2005.

[2] A.S. Kukushkin, H.D. Pacher, V. Kotov, D. Reiter, D. Coster and G.W. Pacher, “Effect of conditions for gas recirculation on divertor operation in ITER”, Nucl. Fusion, vol. 47(7), 2007.

[3] V. Hauer, Chr. Day, “ITER divertor gas flow modelling”, FED, vols. 98-99, pp. 1775-1778, 2015.

[4] R. Wenninger et al., “The physics and technology basis entering European system code studies for DEMO”, Nucl. Fus., vol. 57, pp. 016011, 2017

[5] S. Varoutis et al., “Simulation of neutral gas flow in the JET sub-divertor”, FED, vol. 121, pp. 13-21, 2017.

[6] G. A. Bird, Molecular Gas Dynamics and the Direct Simulation of Gas Flows, Oxford University Press, Oxford, UK, 1994.

[7] F. Bonelli et al., “Self-consistent coupling of DSMC method and SOLPS code for modeling tokamak particle exhaust”, Nucl. Fusion, vol. 57(6), 2017.

[8] S. Varoutis et al., “Optimization of pumping efficiency and divertor operation in DEMO”, Nucl. Materials and Energy, doi:10.1016/j.nme.2017.04.001, 2017.

[9] Chr. Day, S. Varoutis and Yu. Igitkhanov, “Effect of the dome on the collisional neutral gas flow in the DEMO divertor”, IEEE Trans. Plasma Sc., vol. 44(9), 2016.

[10] A.S. Kukushkin, H.D. Pacher, V. Kotov, D. Reiter, D. Coster and G.W. Pacher, “Effects of the dome on divertor performance in ITER“, J. Nucl. Mater., vols. 363-365, pp. 308-313, 2007.

[11] V. Kotov, “Numerical study of the ITER divertor plasma with the B2-EIRENE code package”, Phd Thesis, FZ Jülich, Germany, 2007.